



# Surface morphological modification of crosslinked hydrophilic co-polymers by nanosecond pulsed laser irradiation



Gastón A. Primo<sup>a</sup>, Cecilia I. Alvarez Igarzabal<sup>a</sup>, Gustavo A. Pino<sup>b</sup>, Juan C. Ferrero<sup>b</sup>, Maximiliano Rossa<sup>b,\*</sup>

<sup>a</sup> IMBIV (CONICET), Departamento de Química Orgánica, Facultad de Ciencias Químicas, Universidad Nacional de Córdoba, Haya de la Torre y Medina Allende, Edificio de Ciencias II, Ciudad Universitaria, Córdoba X5000HUA, Argentina

<sup>b</sup> INFIQC (CONICET), Departamento de Fisicoquímica, Facultad de Ciencias Químicas, and Centro Láser de Ciencias Moleculares, Universidad Nacional de Córdoba, Córdoba X5000IUS, Argentina

## ARTICLE INFO

### Article history:

Received 7 December 2015

Received in revised form 3 February 2016

Accepted 4 February 2016

Available online 6 February 2016

### Keywords:

Surface morphological modification  
UV–vis nanosecond pulsed laser irradiation  
Laser ablation craters  
Laser foaming  
Crosslinked hydrophilic co-polymers  
Swell/dried hydrogels

## ABSTRACT

This work reports an investigation of the surface modifications induced by irradiation with nanosecond laser pulses of ultraviolet and visible wavelengths on crosslinked hydrophilic co-polymeric materials, which have been functionalized with 1-vinylimidazole as a co-monomer. A comparison is made between hydrogels differing in the base co-monomer (N,N-dimethylaminoethyl methacrylate and N-[3-(dimethylamino)propyl] methacrylamide) and in hydration state (both swollen and dried states). Formation of craters is the dominant morphological change observed by ablation in the visible at 532 nm, whereas additional, less aggressive surface modifications, chiefly microfoams and roughness, are developed in the ultraviolet at 266 nm. At both irradiation wavelengths, threshold values of the incident laser fluence for the observation of the various surface modifications are determined under single-pulse laser irradiation conditions. It is shown that multiple-pulse irradiation at 266 nm with a limited number of laser shots can be used alternatively for generating a regular microfoam layer at the surface of dried hydrogels based on N,N-dimethylaminoethyl methacrylate. The observations are rationalized on the basis of currently accepted mechanisms for laser-induced polymer surface modification, with a significant contribution of the laser foaming mechanism. Prospective applications of the laser-foamed hydrogel matrices in biomolecule immobilization are suggested.

© 2016 Elsevier B.V. All rights reserved.

## 1. Introduction

The laser-assisted modification of polymeric materials using nanosecond (ns) laser pulses can be currently carried out with high precision and specificity [1,2]. Laser ablation, i.e., the massive removal of polymeric material is the most prevalent result from ns laser-matter interactions at fluences well above the threshold for surface modification. Precise laser processing usually requires the use of ultraviolet (UV) laser wavelengths in order to avoid thermal effects degrading the quality of the modified surface morphologies, as arising from the use of visible (Vis) and infrared (IR) wavelengths [1,3]. Since 2005, a distinct phenomenon, so-called “laser foaming”, has been reported to occur in self-standing films of polymers and biopolymers obtained by casting procedures [4,5]. In laser

foaming, the absorption of a single UV laser pulse of ns duration produces a layer of foamy material featuring bubbles or pores of micro- to nanometric size at the surface of the films. From a practical point of view, such porous morphologies, having high surface areas, find widespread technological applications such as the fabrication of artificial biocompatible extracellular matrices or scaffolds for culture and growth of biological tissue [6,7]. From a fundamental viewpoint, the foaming process unveils a higher level of specificity in the underlying mechanism whereby the laser energy deposited on the film surface ultimately leads to a morphological modification, as compared to regular laser ablation [5].

In general, the mechanism governing the laser foaming of polymers is determined by the laser wavelength, the physical condition of the substrate and its water content [8]. Modeling of the laser foaming process shows up that it is relevant for moderately absorbing polymers, with absorption coefficients  $\alpha < 3000 \text{ cm}^{-1}$  [5]. In such cases, photon absorption from a ns laser pulse at the polymer surface may generate a pressure wave, the tensile part of which is, in

\* Corresponding author.

E-mail address: [mrossa@fcq.unc.edu.ar](mailto:mrossa@fcq.unc.edu.ar) (M. Rossa).

turn, capable of triggering a cavitation and bubbling phenomenon leading to formation of a foam layer. This model proved suitable to account for the foaming characteristics induced by different laser irradiation wavelengths, from UV to IR, on a variety of natural and synthetic polymers from renewable resources [4–6,8–10]. As the matrices of such polymers were prepared by polymer solution casting and further solvent evaporation, without the use of crosslinking agents, they typically had a random association at the molecular level. In the case of collagen, it was demonstrated that UV laser light was capable of inducing conformational changes in the irradiated films, mainly as a result of breaking of the hydrogen bond network and loss of water molecules, which maintain the ordered structure [11]. In few studies on crosslinked gelatin films, the investigations were only limited to dried matrices [8,9]. Significantly so far, there is no research on laser-induced foaming on hydrophilic co-polymeric matrices.

Hydrogels are three-dimensional polymer networks with a unique ability to retain a large amount of water in their swollen state because of the hydrophilic nature of their functional groups [12]. In order to use hydrogels as scaffolds for tissue engineering, their various properties, including porosity and microarchitecture, need to be controlled [13]. In this context, the laser-induced foaming can be used as a post-synthesis technique to increase surface microporosity, and then, diffusion and transport through hydrogels. The present article reports a study of the morphology arising from surface modifications of functionalized hydrogels, as a result of ns pulsed laser irradiation with UV and Vis radiation (266 and 532 nm, respectively). The hydrogels of interest are constituted by N,N-dimethylaminoethyl methacrylate (DMAEMT) and N-[3-(dimethylamino)propyl] methacrylamide (DMAPMD) as monovinyl monomers, 1-vinylimidazole (VI) as a co-monomer, and N,N'-methylenebis(acrylamide) (BIS) as a crosslinking agent. The choice was made on the basis of a recent work in which the synthesis and physicochemical characterization of such crosslinked hydrophilic co-polymers with different proportions of VI was reported [14]. Among them, products containing 20% of VI, designated as MT and MD, were selected because of their largest swelling/resistance ratio in relation to the total materials produced.

Here, the main goal was to find the experimental conditions for the development of surface morphologies, other than regular ablation craters, with emphasis on the generation of a microfoam layer on the surface of the selected hydrogels, in both swollen and dried states. The formation of craters was the dominant morphological change observed by ablation at 532 nm (Vis), whereas additional, less aggressive surface modifications, chiefly microfoams and roughness, were developed at 266 nm (UV). At both irradiation wavelengths, threshold values of the incident laser fluence for the observation of the various surface modifications were determined under single-pulse laser irradiation conditions. The development of surface microfoams on dried MT samples was studied in additional, multiple-pulse experiments at 266 nm with a limited number of laser shots, which allowed a comparison with the foam properties arising from single-pulse irradiation at the foaming threshold fluence.

The observation of ns laser-induced foaming upon UV laser irradiation of functionalized hydrophilic co-polymers is relevant considering the capability of the imidazole group (into VI) to act as a ligand to coordinate a number of transition metal ions eventually dissolved in the swelling water, which in turn can serve as specific sites for the complexation of biomolecules within the hydrogel network [14]. Because such surface-modified morphologies feature micrometric pores or cavities, laser foaming can thus be envisaged as a prospective, post-synthesis strategy to increase the ability of relevant hydrogels for biomolecule immobilization.

## 2. Materials and methods

### 2.1. Reagents and hydrogel synthesis

The following chemicals were used as purchased: DMAEMT (Sigma); DMAPMD (Aldrich); VI (Aldrich); BIS (Sigma); ammonium persulphate (APS, Anedra); and N,N,N',N'-tetramethylethylenediamine (TEMED; Anedra). The hydrogel synthesis procedure, via free-radical crosslinking polymerization, was recently reported [14]. Here,  $4.48 \times 10^{-3}$  mol of monovinyl monomers (DMAEMT or DMAPMD),  $1.12 \times 10^{-3}$  mol of comonomer (VI) and  $1.1 \times 10^{-3}$  mol of crosslinker (BIS) were used. The polymerization reaction was allowed to occur in 5 cm in diameter plastic Petri plates featuring an air-exposed surface, where the defects arising from mold-release processes were absent. After one-day reaction at room temperature, the disk-shaped hydrogels were cut in squares with a  $\sim 1$  cm side using a blade. Square samples were thoroughly washed with Milli-Q water and then dried for two days at 28 °C until constant weight. The final products were named *dr* (meaning for dried) MD and *dr* MT hereafter, to reflect both water content and molar co-monomer composition; upon swelling, the resulting matrices were renamed as *sw* (meaning for swollen) MD and *sw* MT.

The water strongly retained on *dr* MD and *dr* MT samples was 2.86 and 9.60 wt%, respectively. For *sw* MD and *sw* MT, the swelling indexes, as defined by the ratio between the mass of water-swollen hydrogel at equilibrium and the dry mass, were 14 and 30, respectively [14].

### 2.2. Laser irradiation

Laser irradiation of *dr* and *sw* samples of MD and MT was performed in air at room temperature by the second and fourth harmonics (532 and 266 nm, respectively) of a Q-switched Nd:YAG laser (Big Sky Laser-Quantel CFR 400, 6 ns FWHM). In the case of *sw* samples, the water from the surfaces was removed prior to laser irradiation by wiping with tissue paper. Single laser pulses were isolated manually from the output of the laser working at a repetition rate of 2 Hz. The laser output was steered using a quartz prism on the hydrogel samples, which had been placed horizontally on a two-dimensional micrometric translation stage and focused by a plano-convex lens (Thorlabs, quartz, 10 cm focal length) onto the sample surface at normal incidence.

The cross-section of the laser beam at the focal plane *A* was estimated from digital analysis of confocal laser microscope (CLM) images of the burned pattern on photosensitive papers. The CLM used was Olympus LEXT – OLS 4100. The laser output power was controlled in order to keep the incident laser pulse energy  $E_p$  at values below 20.0 and 3.5 mJ, at 532 and 266 nm, respectively, as measured by placing a Scientech 756 calorimetric detector right behind the focusing lens. The incident laser fluence  $\phi$ , as applicable to single-pulse irradiation experiments, was estimated by the  $E_p$  to *A* ratio [15,16]. For multiple-pulse irradiation experiments on *dr* MT, recording the effect of an accumulative number  $N=2-5$  of laser pulses applied to the same area,  $\phi$  was set to the value of the corresponding single-pulse threshold fluence for laser foaming (see below), to yield effective energy doses of  $(N.\phi)$ .

For the sake of reproducibility, the laser irradiation under both single- and multiple-pulse conditions was carried out on two different samples in any given assay combining type and state of hydrogel and laser wavelength.

### 2.3. Confocal laser microscopy and scanning electron microscopy

The morphology of the irradiated areas of *dr* samples was characterized using the CLM and a scanning electron microscope (SEM);

Carl Zeiss FE-SEM Sigma), whereas *sw* samples were evaluated only by CLM. The estimation for surface roughness, via mean roughness ( $R_a$ ) parameter, and for surface pore mean density and area was obtained from digital analysis of CLM and SEM images. The  $R_a$  values represent the arithmetic average of the deviations from the center plane of the sample. Each  $R_a$  value corresponds to the average of three independent measurements in different locations of the matrix surface.

#### 2.4. UV–vis spectroscopy

Further characterization of the hydrogels was carried out by measuring their UV–vis absorption spectra between 250 and 800 nm using a StellarNet Black-Comet (BLK-CXR-SR) spectrometer.

### 3. Results

Fig. 1 compares the UV–vis absorption spectra of MT and MD, in both *sw* and *dr* states, with those corresponding to monomers ( $1 \times 10^{-3}$  M aqueous solutions of DMAEMT; DMAPMD; BIS and VI). For all matrices, negligible absorbance is observed at wavelengths above 500 nm, whereas absorbance of the laser radiation at 266 nm can be ascribed to the chromophores present in the structure of the hydrogels, i.e., the imidazole ring in VI and the carbonyl groups in DMAEMT, DMAPMD and BIS. Table 1 lists the derived attenuation coefficients for the hydrogels. Apparently, the polymers feature

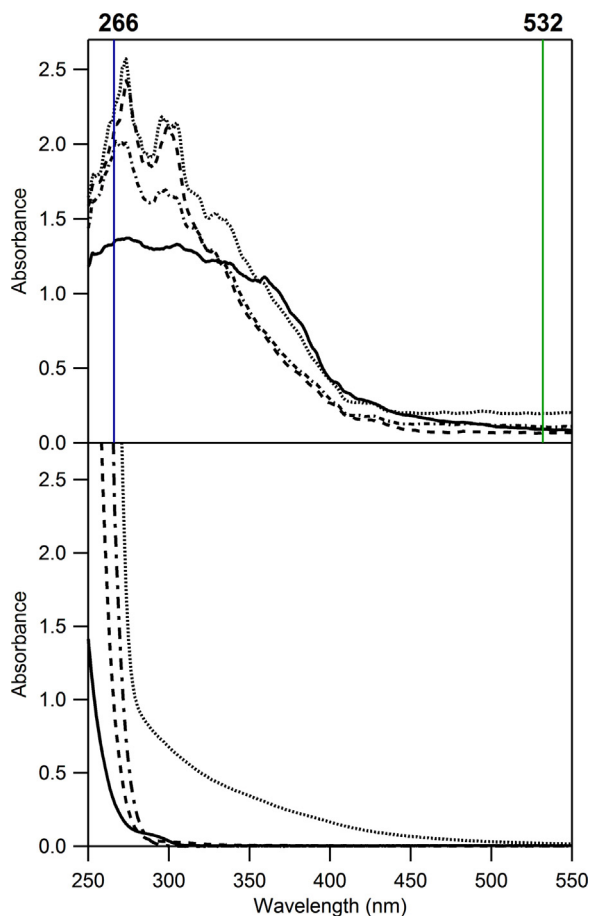


**Fig. 1.** Upper panel: UV–vis absorption spectra of the hydrogels before laser irradiation. *dr* MT (—), *dr* MD (---), *sw* MT (— · —), and *sw* MD (····). Lower panel: UV–vis absorption spectra of diluted aqueous solutions of the monomers. DMAEMT (—), DMAPMD (---), BIS (— · —), and VI (····).

**Table 1**

Attenuation coefficients  $\alpha$  (in  $\text{cm}^{-1}$ ) at the wavelengths used for pulsed laser irradiation,  $\lambda_{\text{LI}}$ .

Hydrogel		$\lambda_{\text{LI}}$ (nm)	$\alpha^a$
Type	Hydration state		
MT	Dried	266	20
	Swollen	266	12
MD	Dried	266	15
	Swollen	266	14
MT	Dried	532	1
	Swollen	532	1
MD	Dried	532	1
	Swollen	532	1

<sup>a</sup> As derived from the spectra in Fig. 1 and thickness of the hydrogels: 1.04 for *dr* MT, 0.88 for *dr* MD, 1.60 for *sw* MT, and 1.62 mm for *sw* MD.

**Table 2**

Threshold incident laser fluences  $\phi$  (in  $\text{J cm}^{-2}$ ; uncertainties in parentheses) for the observed surface modifications of the hydrogels at both laser irradiation wavelengths, as applicable to single-pulse irradiation experiments.

Hydrogel		$\lambda_{\text{LI}}^a$ (nm)	$\phi_R^b$	$\phi_F^c$	$\phi_A^d$	
Type	State					
MT	Dried	266	–	0.9 (0.1)	–	
	Swollen	Dried	532	–	3.4 (0.3)	
		Dried	266	–	1.0 (0.1) <sup>f</sup>	
		Swollen	532	–	1.1 (0.1) <sup>f</sup>	
MD	Dried	266	–	2.3 (0.3)	–	
	Swollen	Dried	532	–	4.6 (0.4)	
		Dried	266	4.6 (0.5)	–	5.1 (0.5)
		Swollen	532	–	–	3.2 (0.3)

<sup>a</sup> Pulsed laser irradiation wavelength.

<sup>b</sup>  $R$  = roughness.

<sup>c</sup>  $F$  = foaming.

<sup>d</sup>  $A$  = ablation.

<sup>e</sup> Upper value: threshold for irregular foaming (with concurrent development of surface roughness); lower value (in brackets): threshold for regular foaming.

<sup>f</sup> Craterization with concurrent development of additional morphology (see text).

relatively low attenuation coefficients even at the laser irradiation wavelength of 266 nm.

The single-pulse ns laser irradiation of the hydrogels at 266 and 532 nm showed a variety of morphological modifications in the surfaces including the development of roughness, microfoams and ablation craters. For the various assays combining type and state of hydrogel and laser wavelength, threshold fluences were determined by measuring minimum fluence, leading to any particular morphological alteration in the sample surfaces, as probed by CLM. Table 2 lists such threshold fluence values. Fig. 2 shows typical CLM images of the irradiated regions of the relevant samples at laser fluences above their lowest-lying thresholds.

From the evidence, it is apparent that the irradiation at 266 nm of *dr* MT and *dr* MD leads to development of foam-like morphologies within the irradiated areas under the prevailing experimental conditions. At fluences above 2.1 and 2.3  $\text{J cm}^{-2}$  for *dr* MT and *dr* MD, respectively, such microfoams feature regular distributions of micrometer-sized cavities or pores (Fig. 3). They were correspondingly characterized by pore mean areas of 0.092 and 0.025  $\mu\text{m}^2$ , as well as pore densities of  $1.61 \times 10^6$  and  $4.44 \times 10^6$  pore  $\text{mm}^{-2}$  at fluences of 2.1 and 4.1  $\text{J cm}^{-2}$ , respectively. For *dr* MT, a fluence range was found, from the foaming threshold at 0.9  $\text{J cm}^{-2}$  to 2.1  $\text{J cm}^{-2}$ , in which irregular microfoams developed, showing a steady increase in pore density with fluence. In addition, a varying depth of the open cavities under the surface is observed at any given fluence (Fig. 4). Concurrently, the irradiated area increases in surface

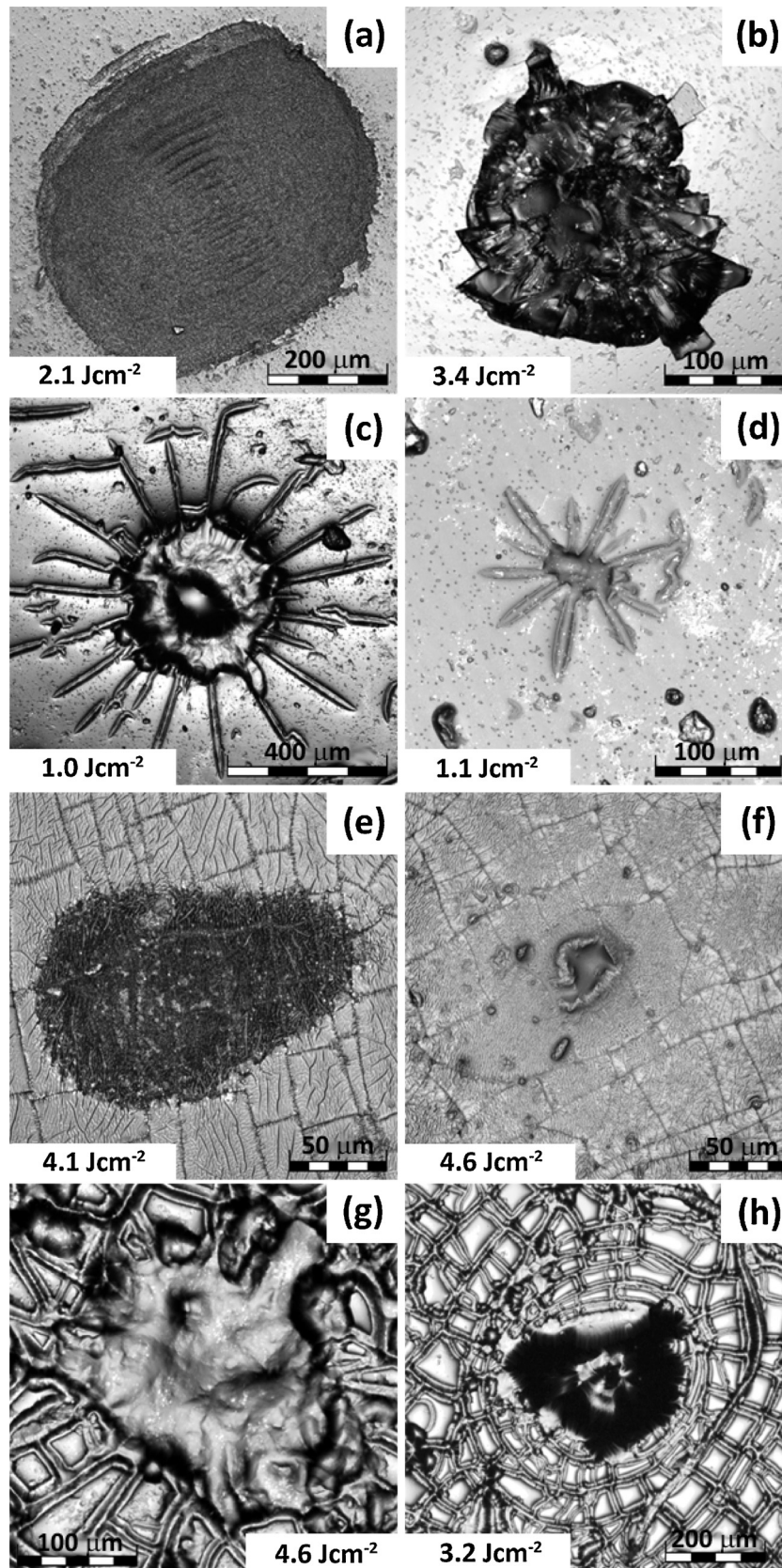


**Fig. 2.** CLM images of the surface morphologies of the hydrogels after single-pulse laser irradiation at the laser wavelengths of 266 (left column) and 532 nm (right column) and at the indicated incident laser fluences. (a and b) *dr* MT; (c and d) *sw* MT; (e and f) *dr* MD; (g and h) *sw* MD.



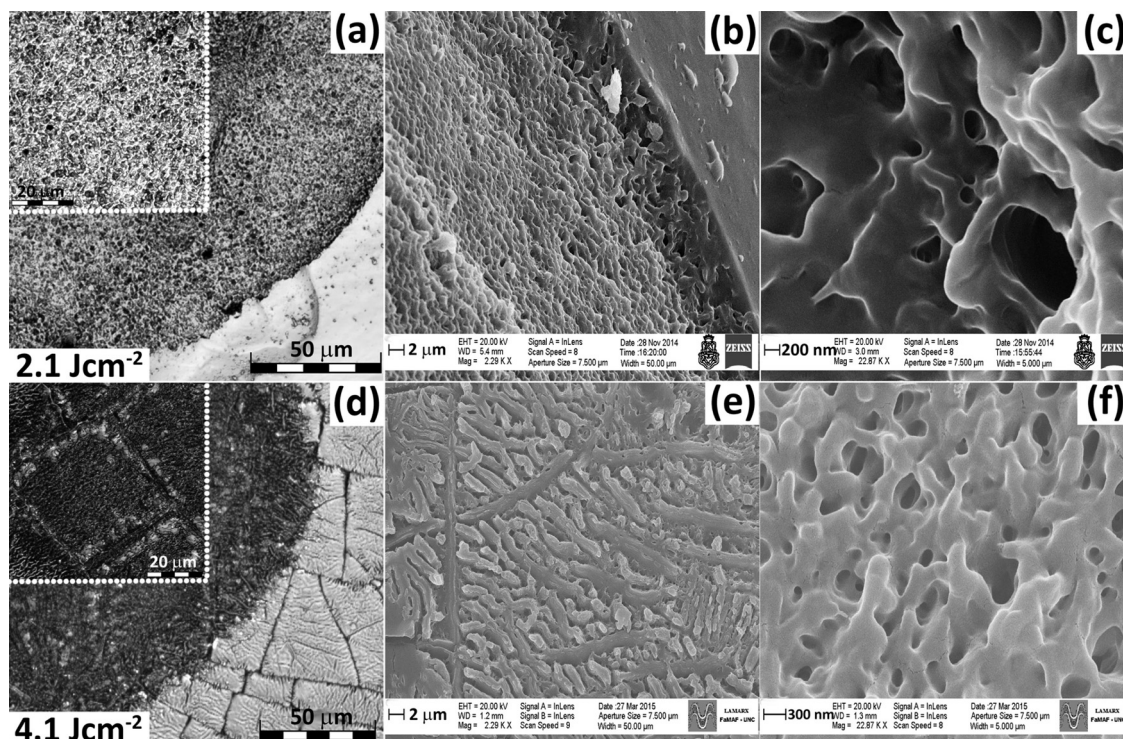


**Fig. 3.** CLM (left column) and SEM (middle and right columns) images of the surface morphologies of *dr* MT (upper panels) and *dr* MD (lower panels) after single-pulse laser irradiation at 266 nm and at the indicated incident laser fluences. (b) is an inclined view showing the depression, as a result of material removal from the irradiated area that accompanies laser foaming of *dr* MT at laser fluences above  $2.1 \text{ J cm}^{-2}$ .

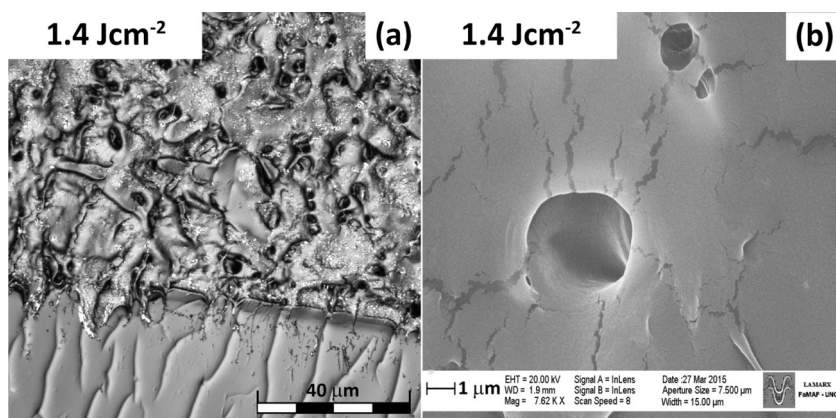


**Fig. 4.** CLM (a) and SEM (b) images of the surface morphologies of *dr* MT after single-pulse laser irradiation at 266 nm and at an incident laser fluence of  $1.4 \text{ J cm}^{-2}$ .

roughness, as evidenced by  $R_a$  changing in the range of  $0.14\text{--}1.0 \mu\text{m}$  from unexposed to irradiated surfaces.

These observations are similar to those reported in previous studies on single-pulse, ns laser irradiation at 248 and 266 nm of thin films of biopolymers and polymers from renewable resources [4–6,8–10]. A major difference with such studies concerns the lack of swelling in the irradiated area even at near-threshold fluences. The thickness of the foam layer depends on the polymer and  $\phi$ : for instance, it is around 21 and  $4 \mu\text{m}$  for *dr* MT and *dr* MD at  $2.1$  and  $4.1 \text{ J cm}^{-2}$ , respectively. Fig. 5 illustrates it, showing an inclined view of a cross-section of the foam layer for *dr* MD. Noteworthy, such foam-like morphologies are preserved after at least one swelling/deswelling cycle (Fig. S1 of the Supporting Information).

For the other hydrogel states and laser wavelengths, laser irradiation of the samples leads to development of roughness or craters, either individually or sequentially (Table 2). In the case of *sw* MT

at  $\lambda_{LI} = 266$  and  $532 \text{ nm}$ , crater formation is accompanied by the development of two distinct morphologies around the crater. This is chiefly evidenced in Fig. 2(c), where the crater (looking opaque at the CLM image center) is surrounded by a larger, nearly circular plateau with a roughness, which is higher than that of the unexposed regions. Beyond such a plateau, a number of elongated promontories spread radially out, which overall results in a morphology looking like a “sun in splendor”. These promontories are arguable surface fissures (filled with water) derived from a mechanical fracture of the unexposed regions, as the laser-induced momentum [10] within the irradiated area forces the surface to a fast recoil and ensuing swelling with curvatures, exceeding the mechanical resistance of the matrix.

The development of microfoams, resulting from laser irradiation at 266 nm of *dr* MT, was further explored in experiments using an accumulative number  $N$ , from 2 to 5, of laser pulses



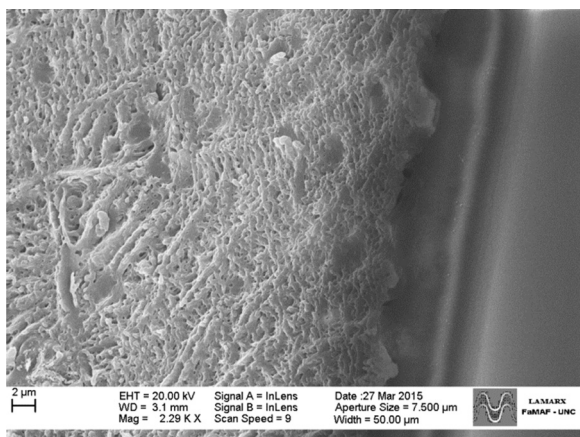


**Fig. 5.** SEM image (with inclined view) of a cross-section of the foam layer resulting from single-pulse laser irradiation of *dr* MD at 266 nm and at an incident laser fluence of  $4.1 \text{ J cm}^{-2}$ .

applied to the same area. The laser fluence was set to a value of  $0.9 \text{ J cm}^{-2}$ , i.e., the corresponding single-pulse threshold fluence for laser foaming. Under such conditions, the generation of a regular pore size distribution required the incidence of 2 shots to yield an effective energy dose of  $1.8 \text{ J cm}^{-2}$ . Significantly, this is below the single-pulse  $\phi$  value of  $2.1 \text{ J cm}^{-2}$  that was found for the development of regular foams on *dr* MT. The microfoams resulting from multiple-pulse irradiation show pore densities that increase from  $1.45 \times 10^4$  to  $9.52 \times 10^4$  pore  $\text{mm}^{-2}$  from  $N=2$  to 5 (Fig. 6). The similarity between these and the foam properties arising from single-pulse experiments suggests that multiple-pulse irradiation at 266 nm with a limited number of laser shots and at fluences near the foaming threshold can be alternatively used to generate a regular microfoam layer on the surface of the hydrogels.

It should be pointed out that the optical properties of the starting (non irradiated) hydrogels, as derived from the spectra in Fig. 1, are not representative of those characterizing the matrices after the incidence of the first and subsequent laser pulses. Such successive shots are expected to increase the concentration within the irradiated volume of laser radiation-induced defects, i.e., the so-called incubation centers [2], thereby resulting in a local increase in absorptivity. Unfortunately, the relatively small area of the microfoams, which arise from multiple-pulse irradiation, prevented further probing of their local optical properties via conventional UV–vis absorption spectroscopy. Yet, the finding in multiple-pulse experiments that regular foams are developed on *dr* MT at an effective energy dose, which is lower than the corresponding single-pulse threshold fluence, is suggestive of the occurrence in the former conditions of incubation phenomena, most likely resulting from a radiation-induced increase in the absorptivity [2].

#### 4. Discussion

The results can be interpreted in terms of the currently accepted mechanisms for ns laser-induced polymer surface modification [1–3,5], with a consideration of the relative optical penetration depths  $l_a$  ( $\equiv \alpha^{-1}$ ) for the various samples at the two  $\lambda_{\text{L}}$ 's. For laser irradiation at 532 nm, either photochemical or photothermal mechanisms would explain the formation of both simple craters for *dr* MT and *dr/sw* MD, and craters with distinct morphologies around for *sw* MT. The corresponding low attenuation coefficients at 532 nm (Table 1) support the major involvement of a laser ablation mechanism, which massively removes polymeric material at relatively large penetration depths [3].

In general, for laser irradiation at 266 nm, there appears to be a contribution from an additional mechanism which leads to morphological changes, more localized on the sample surfaces, in agreement with the expected small penetration depths (i.e., high

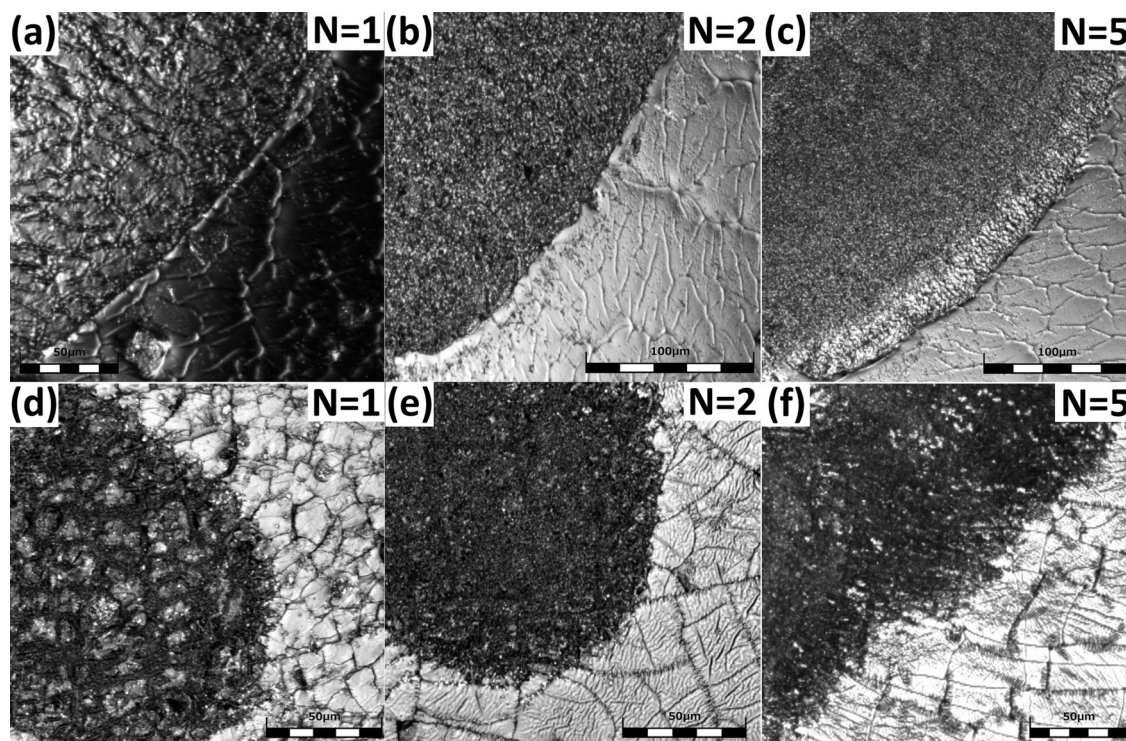


**Fig. 6.** CLM images of the surface morphologies of *dr* MT (upper panels) and *dr* MD (lower panels) after multiple-pulse laser irradiation at 266 nm ( $\phi$ 's of 0.9 and  $2.3 \text{ J cm}^{-2}$ , respectively), at the indicated incident accumulative laser pulses.

**Table 3**  
Physicochemical properties for the starting (non irradiated) hydrogels.<sup>a</sup>

	Hydrogel	
	MT	MD
Density (g mL <sup>-1</sup> )	1.12	1.13
Young's modulus (kPa)	664.4	609.0
Failure strain (kJ mL <sup>-3</sup> )	8542.7	529.6
Decomposition temperature (°C)	197.12/351.07	197.12
Maximum # of swelling/deswelling cycles before material breakdown	16	4

<sup>a</sup> Ref. [14].

attenuation coefficients), in comparison with 532 nm. Lazare and coworkers studied and modeled the foaming process, as induced by ns laser irradiation, of a number of moderately absorbing films of polymers from renewable sources [5]. Within this model, the formation of a foam layer on the polymer surface is initiated by absorption of a single laser pulse, which in turn produces a transient acoustic wave that propagates into the dense material. Such a pressure wave contains both compressive and tensile components, and the latter is thought to be ultimately responsible for fast cavitation and bubble growth. In addition, the water content of the polymer matrix plays a major role in cooling the irradiated surface. Lazare et al. also pointed out [10] the difficulty of discerning laser foaming from laser ablation phenomenon (driven by either photochemical or photothermal mechanisms) on the surface of polymers, due to simultaneous occurrence and varying relative relevance with increasing laser fluence. Therefore, for laser irradiation at 266 nm on dried matrices, the laser foaming mechanism accounts for the formation of superficial microfoams, in addition to the development of surface roughness that accompanies laser foaming on MT at laser fluences in the range of 0.9–2.1 J cm<sup>-2</sup>. In the case of swollen samples at  $\lambda_{LI} = 266$  nm, this model most likely explains the surface roughness that either occurs at lower fluences than the craterization threshold for MD, or accompanies the formation of ablation craters for MT.

In addition, the above mechanisms provide a rationalization for the correlations observed between the threshold fluences for the hydrogels and the variables of the laser irradiation process, like type and state of hydrogel and laser wavelength. The most general trend has been found under single-pulse irradiation conditions (Table 2) at which, for any given hydrogel state and laser wavelength, the threshold fluence for the development of a particular morphology is lower for MT than for MD. For example, the laser-foaming threshold of *dr* MT at  $\lambda_{LI} = 266$  nm (of 0.9 J cm<sup>-2</sup>) is lower than the corresponding value (of 2.3 J cm<sup>-2</sup>) of *dr* MD. Similar considerations can be applied to the relative craterization thresholds of *dr/sw* MT and *dr/sw* MD at the two prevailing  $\lambda_{LI}$ 's.

Table 3 lists a number of physicochemical properties for the hydrogels reported previously [14]. A comparison between Tables 1 and 3 reveals that neither the optical attenuation coefficients at a given  $\lambda_{LI}$  nor the densities of the matrices significantly depend on the identity of the VI's co-monomer, whether DMAEMT or DMAPMD. It is also apparent that DMAEMT-containing matrices show improved mechanical properties in terms of Young's modulus and failure strain, increased thermal stability (higher decomposition temperature) and resistance to a higher number of swelling/deswelling cycles in relation to DMAPMD-containing hydrogels. Such differences in mechanical strength and thermal stability would expectedly result in lower threshold fluences for surface morphological modification in the case of *dr/sw* MD with respect to *dr/sw* MT, which is opposite to observations on single-pulse experiments. A similar behavior has been reported in previous studies on the ns, single-pulse laser irradiation of self-standing gelatin films at UV, Vis and IR laser wavelengths, in which

Bloom 225 gelatin samples consistently displayed lower modification threshold fluences than those of Bloom 75, despite the higher gel strength of the former [8,9].

At  $\lambda_{LI} = 266$  nm, where the foaming mechanism seems to dominate the contributions to the laser-assisted modifications, the explanation most likely relies on the relevance given by the model to the concentration within the hydrogel network of free-volume holes (FVH) [5]. These are regions of the material with zero density of bonds and constitute seeds for the nucleation of cavities and bubbles, which further expand and grow upon the action of the tensile component of the pressure wave. An insight into the relative size of FVH for the relevant crosslinked hydrophilic materials can be obtained from a morphological characterization performed via variable pressure scanning electron microscopy (VP-SEM) technique, which have revealed that the pores of non irradiated *sw* MD matrices are significantly larger than those of *sw* MT [14]. This is in agreement with the estimation of the corresponding values for the hydrogel mesh size  $\xi$  of the swollen matrices, using the proper formulae for non-ionic hydrogels [17], which leads to  $\xi$  values of around 8 and 100 nm for MT and MD, respectively.

Because the pore size ratio of MD to MT is not expected to vary significantly upon the drying process, the preceding conclusions could be expected to hold for dried matrices. Hence, the large difference in pore size between the two matrices, by about one order of magnitude, would result in a higher concentration of FVH for *dr* MT than that for *dr* MD. Within the laser foaming mechanism [5], the nucleation rate of cavities is proportional to the concentration of FVH in the starting polymer, which in turn would imply that *dr* MT is more prone to the foaming process than *dr* MD under similar conditions. This is in agreement with the above-mentioned correlations between the type of hydrogels and threshold fluences. At  $\lambda_{LI} = 266$  nm, this is supported by the larger pore mean areas and smaller pore densities, which characterize the microfoams of *dr* MT, compared to those of *dr* MD, suggesting that laser-induced polymer surface modification takes place, to a larger extent, for the former. At  $\lambda_{LI} = 532$  nm, where either photochemical or photothermal mechanisms are predicted to dominate the polymeric material removal, such an agreement is indicative of a significant contribution of the laser foaming mechanism as well.

Only a partial correlation can be found between hydrogel state and threshold fluences for the hydrogels. For the two types of copolymers at  $\lambda_{LI} = 532$  nm, it was observed that their craterization thresholds are lower for swollen than for dried matrices. No correlation is instead apparent at  $\lambda_{LI} = 266$  nm, which could partly be due to the different morphologies developed, e.g., microfoams on *dr* MT and craters on *sw* MT. Yet, an involvement of the laser foaming mechanism could be inferred from the mechanical fractures observed around craters at the surface of *sw* MT for  $\lambda_{LI} = 266$  and 532 nm. Hence, such fractures were possible due to the low polymer tensile strength of swollen matrices with large water content, as compared to that of dried samples. The absence of mechanical fractures for *sw* MD under similar laser irradiation conditions could be the result of a lower propensity for these matrices to undergo laser foaming.

No trend is observed addressing the effect of laser wavelength on the fluence thresholds for any given type and state of hydrogel; once again, this could reflect the different morphologies developed upon changing  $\lambda_{LI}$ .

## 5. Conclusions

This work shows that ns, single-pulse laser irradiation of crosslinked hydrophilic co-polymers at a UV wavelength (266 nm) and at relatively low laser fluences allowed producing surface modifications, other than ablation craters, especially microfoam layers



with a regular size distribution of pores. It was also concluded that multiple-pulse irradiation at 266 nm with a limited number (2–5) of laser shots can be used alternatively for generating a regular microfoam layer at the surface of *dr* MT. These results parallel findings previously made in experimental studies on the laser foaming process in films of biopolymers and polymers from renewable sources, which typically show polymer structures with a random association at the molecular level. Foamy morphologies, as induced on dried samples of MT and MD, proved to resist at least one swelling/deswelling cycle without significant degradation. Instead, single-pulse laser irradiation in the visible at 532 nm led preferentially to crater formation on the hydrogel surfaces.

At the two irradiation wavelengths, the incident laser fluence dependences of the observed surface modifications have further been recorded, which allowed for a determination of the corresponding threshold fluences under single-pulse laser conditions. Significantly, a marked correlation was found between the type of hydrogel and the various threshold fluences: for any given hydrogel state and laser wavelength, the threshold fluence for the development of a particular morphology is consistently lower for MT than for MD.

The most important features of the various surface morphological modifications arising from laser irradiation at 266 and 532 nm were rationalized in terms of the currently accepted mechanisms for ns laser-induced polymer surface modification. The laser foaming mechanism was proposed to dominate the contribution at the UV wavelength, whereas either photochemical or photothermal mechanisms favoring regular laser ablation could additionally be involved, or even dominate at 532 nm.

Laser-foamed dry matrices of MT and MD appear as suitable precursors for prospective studies on better ability (upon subsequent swelling) for biomolecule immobilization. These applications would benefit from additional, complementary investigations of the chemical changes in the hydrogel structure, which accompany the surface morphological modifications reported here. Such a knowledge is important for the present systems considering that the immobilization of biomolecules, within the hydrogel network, is expected to occur through complexation with transition metal ions (suitably dissolved in the swelling water), which can concurrently coordinate to the imidazole groups of the VI's constituents. A great deal of information on the chemical and conformational changes, which ensue the development of laser-induced microfoams on hydrophilic polymers, can be attained through a number of spectroscopic techniques including laser-induced fluorescence (LIF) [6,9,18], time-correlated single photon counting (TCSPC) fluorescence spectroscopy [18], Raman spectroscopy [11], Fourier transform infrared spectroscopy in attenuated total reflection mode (FTIR-ATR) [11,19], and X-ray photoelectron spectroscopy (XPS) [19]. Such spectroscopic studies will be the subject of a forthcoming investigation.

## Acknowledgments

Financial support from CONICET (PIP No. 11220120100331), FONCyT (PICT-2013-0311 and PICT-2011-0654), SeCyT-UNC (05/C667 and 203/14) and MinCyT Córdoba is acknowledged. G.A. Primo also acknowledges receipt of a fellowship from CIN.

## Appendix A. Supplementary data

Supplementary data associated with this article can be found, in the online version, at <http://dx.doi.org/10.1016/j.apsusc.2016.02.047>.

## References

- [1] M. Castillejo, P. Ossi, L. Zhigilei (Eds.), *Lasers in Materials Science*, Springer Series in Materials Science 191, Springer International Publishing, Switzerland, 2014.
- [2] D. Bäuerle, *Laser Processing and Chemistry*, Springer-Verlag, Berlin, 2000.
- [3] P.F. Conforti, M. Prasad, B.J. Garrison, Elucidating the thermal, chemical, and mechanical mechanisms of ultraviolet ablation in poly(methyl methacrylate) via molecular dynamics simulations, *Acc. Chem. Res.* 41 (2008) 915–924.
- [4] S. Lazare, V. Tokarev, A. Sionkowska, M. Wiśniewski, Surface foaming of collagen, chitosan and other biopolymer films by KrF excimer laser ablation in the photomechanical regime, *Appl. Phys. A* 81 (2005) 465–470.
- [5] S. Lazare, I. Elaboudi, M. Castillejo, A. Sionkowska, Model properties relevant to laser ablation of moderately absorbing polymers, *Appl. Phys. A* 101 (2010) 215–224.
- [6] M. Castillejo, E. Rebollar, M. Oujja, M. Sanz, A. Selimis, M. Sigletou, S. Psycharakis, A. Ranella, C. Fotakis, Fabrication of porous biopolymer substrates for cell growth by UV laser: the role of pulse duration, *Appl. Surf. Sci.* 258 (2012) 8919–8927.
- [7] A. Daskalova, C.S.R. Nathala, I. Bliznakova, E. Stoyanova, A. Zhelyazkova, T. Ganz, S. Lueftenegger, W. Husinsky, Controlling the porosity of collagen, gelatin and elastin biomaterials by ultrashort laser pulses, *Appl. Surf. Sci.* 292 (2014) 367–377.
- [8] M. Castillejo, M. Oujja, E. Rebollar, S. Gaspard, C. Abrusci, F. Catalina, S. Lazare, Submicron foaming in biopolymers by UV pulsed laser irradiation, *Proc. SPIE High-Power Laser Ablation VI*, vol. 6261 (2006) 62611L.
- [9] M. Oujja, E. Rebollar, C. Abrusci, A. del Amo, F. Catalina, M. Castillejo, UV, visible and IR laser interaction with gelatine, *J. Phys. Conf. Ser.* 59 (2007) 571–574.
- [10] S. Lazare, A. Sionkowska, M. Zaborowicz, A. Planecka, J. Lopez, M. Dijoux, C. Louména, M.-C. Hernandez, Bombyx mori silk protein films microprocessing with a nanosecond ultraviolet laser and a femtosecond laser workstation: theory and experiments, *Appl. Phys. A* 106 (2012) 67–77.
- [11] M. Wisniewski, A. Sionkowska, H. Kaczmarek, S. Lazare, V. Tokarev, C. Belin, Spectroscopic study of a KrF excimer laser treated surface of the thin collagen films, *J. Photochem. Photobiol. A: Chem.* 188 (2007) 192–199.
- [12] S.J. Buwalda, K.W.M. Boere, P.J. Dijkstra, J. Feijen, T. Vermonden, W.E. Hennink, Hydrogels in a historical perspective: from simple networks to smart materials, *J. Control. Release* 190 (2014) 254–273.
- [13] N. Annabi, J.W. Nichol, X. Zhong, C. Ji, S. Koshy, A. Khademhosseini, F. Dehghani, Controlling the porosity and microarchitecture of hydrogels for tissue engineering, *Tissue Eng.: Part B* 16 (2010) 371–383.
- [14] G.A. Primo, M.F. Garcia Manzano, M.R. Romero, C.I. Alvarez Igarzabal, Synthesis and characterization of hydrogels from 1-vinylimidazole. Highly resistant co-polymers with synergistic effect, *Mater. Chem. Phys.* 153 (2015) 365–375.
- [15] I. Cabanillas-Vidosa, C.A. Rinaldi, J.C. Ferrero, Optical emission and mass spectrometric characterization of laser ablation process of Ca, Mg, and Ba at 1064 nm, *J. Appl. Phys.* 102 (2007) 0131101–131107.
- [16] M. Rossa, C.A. Rinaldi, J.C. Ferrero, Internal state populations and velocity distributions of monatomic species ejected after the 1064 nm laser irradiation of barium, *J. Appl. Phys.* 105 (2009) 0633061–633113.
- [17] N. Milašinović, N. Milosavljević, J. Filipović, Z. Knežević-Jugović, M. Kalagasić Krušić, Synthesis, characterization and application of poly(N-isopropylacrylamide-co-itaconic acid) hydrogels as supports for lipase immobilization, *React. Funct. Polym.* 70 (2010) 807–814.
- [18] S. Gaspard, M. Oujja, C. Abrusci, F. Catalina, S. Lazare, J.P. Desvergne, M. Castillejo, Laser induced foaming and chemical modifications of gelatine films, *J. Photochem. Photobiol. A: Chem.* 193 (2008) 187–192.
- [19] Zainuddin, T.V. Chirila, Z. Barnard, G.S. Watson, C. Toh, I. Blakey, A.K. Whittaker, D.J.T. Hill, F<sub>2</sub> excimer laser (157 nm) radiation modification and surface ablation of PHEMA hydrogels and the effects on bioactivity: surface attachment and proliferation of human corneal epithelial cells, *Radiat. Phys. Chem.* 80 (2011) 219–229.